Published in final edited form as:
Stem Cells. 2014 July ; 32(7): 1831–1842. doi:10.1002/stem.1676.

Human adipose derived stromal/stem cells (hASCs) protect against STZ-induced hyperglycemia; analysis of hASC-derived paracrine effectors

Tatsuyoshi M. Kono, Ph.D.[1], **Emily K. Sims, M.D.**[2], **Dan R. Moss, B.S.**[1], **Wataru Yamamoto, B.S.**[3], **Geonyoung Ahn, M.S.**[6], **Julie Diamond, B.S.**[6], **Xin Tong, B.S.**[3], **Kathleen H. Day, M.S.**[1], **Paul R. Territo, Ph.D.**[4], **Helmut Hanenberg, M.D.**[2,6], **Dmitry O. Traktuev, Ph.D.**[1], **Keith L. March, M.D., Ph.D.**[1], and **Carmella Evans-Molina, M.D. Ph.D.**[1,3,5,6]

[1]Department of Medicine, Indiana University School of Medicine, Indianapolis IN, USA

[2]Department of Pediatrics, Indiana University School of Medicine, Indianapolis IN, USA

[3]Department of Cellular and Integrative Physiology, Indiana University School of Medicine, Indianapolis IN, USA

[4]Department of Radiology and Imaging Sciences, Indiana University School of Medicine, Indianapolis IN, USA

[5]Department of Biochemistry and Molecular Biology, Indiana University School of Medicine, Indianapolis IN, USA

[6]Herman B Wells Center for Pediatric Research, Indiana University School of Medicine, Indianapolis IN, USA

Abstract

Adipose-derived stromal/stem cells (ASCs) ameliorate hyperglycemia in rodent models of islet transplantation and autoimmune diabetes, yet the precise human ASC (hASC)-derived factors responsible for these effects remain largely unexplored. Here, we show that systemic administration of hASCs improved glucose tolerance, preserved β cell mass, and increased β cell proliferation in STZ-treated NOD-SCID mice. Co-culture experiments combining mouse or human islets with hASCs demonstrated that islet viability and function were improved by hASCs following prolonged culture or treatment with pro-inflammatory cytokines. Analysis of hASC-

Address correspondence and requests for reprints to: Carmella Evans-Molina, Indiana University School of Medicine, 635 Barnhill Drive, MS 2031A, Indianapolis, IN 46202, cevansmo@iu.edu, Telephone: (317) 274-4145, Fax (317) 274-4107.

The authors have no relevant conflicts of interest to disclose

AUTHOR CONTRIBUTIONS

Tatsuyoshi M. Kono and Emily K. Sims: participated in the conception and design of the study, data analysis and interpretation, collection and assembly of data, manuscript writing, and final approval of manuscript.
Dan R. Moss, Wataru Yamamoto, Geonyoung Ahn, Julie Diamond, Xin Tong, Kathy Day: participated in collection of data and final approval of the manuscript.
Dmitry O. Traktuev and Keith L. March: participated in study conception and participated in the final approval of the manuscript.
Paul R. Territo: participated in study design and data analysis and interpretation and provided final approval of the manuscript.
Helmut Hanenberg: provided study material and provided final approval of the manuscript.
Carmella Evans-Molina: directed the conception and design, provided financial support, participated in the collection and assembly of data, data analysis and interpretation, manuscript writing, and final approval of the manuscript.

derived factors revealed VEGF and TIMP-1 to be highly abundant factors secreted by hASCs. Notably, TIMP-1 secretion increased in the presence of islet stress from cytokine treatment, while TIMP-1 blockade was able to abrogate *in vitro* pro-survival effects of hASCs. Following systemic administration by tail vein injection, hASCs were detected in the pancreas and human TIMP-1 was increased in the serum of injected mice, while recombinant TIMP-1 increased viability in INS-1 cells treated with IL-1β, IFN-γ and TNF-α. In aggregate, our data support a model whereby factors secreted by hASCs, such as TIMP-1, are able to mitigate against β cell death in rodent and *in vitro* models of Type 1 diabetes through a combination of local paracrine as well as systemic effects.

Keywords

diabetes; adipose stem cells; pancreas; caspase; cellular proliferation; tissue regeneration

Type 1 diabetes mellitus (T1DM) is a disease in which the insulin-secreting islet β cells are destroyed through a T cell mediated immune response. T1DM affects nearly 3 million individuals in the U.S. and is currently the third most common chronic health condition among American youth with an estimated annual cost of $14.4 billion [1–3]. Though the cause is unclear, the worldwide incidence of this disease is increasing at a rate of approximately 3% per year [4, 5]. Insulin therapy is able to regulate blood glucose levels within fairly narrow ranges, yet persons with T1DM are still at significantly increased risk of developing microvascular and macrovascular disease-associated complications [6, 7]. Transplantation of either whole pancreata or isolated islets is potentially curative, however organ availability limits the widespread application of these therapies. Furthermore, long-term rates of insulin independence from either method remain imperfect [8, 9].

Stem cell-based therapies are being increasingly explored as a novel and potentially curative strategy for the treatment of T1DM. Methods to differentiate embryonic, induced pluripotent, or adult stem cells into engineered β cells are ongoing and offer the possibility of a renewable source of insulin producing cells [10]. In preclinical models, systemic or local administration of allogeneic or syngeneic adult stems cells, such as bone marrow-derived mesenchymal stem cells (MSCs), have shown beneficial effects on the prevention or reversal of autoimmune and chemical-induced diabetes [11–13]. Recently, adipose stromal tissue has emerged as a promising source of MSCs with regenerative and potentially immunosuppressive characteristics. Adipose derived stem cells (ASCs) isolated from the stromal vascular fraction of fat are easily accessible through liposuction procedures. These cells can be expanded *in vitro*, and their procurement is associated with minimal patient risk. ASCs have been shown to aid in tissue repair in a number of disease models [14–18]. As companion cells in rodent transplantation strategies, ASCs promote islet graft survival and revascularization [19]. Recently, intraperitoneal administration of murine-derived ASCs to diabetic non-obese diabetic (NOD) mice also decreased hyperglycemia and insulitis through attenuation of the Th1 immune response and expansion of T regulatory lymphocytes [20]. While these reports support a therapeutic role for ASCs in T1DM, the precise human ASC (hASC)-derived factors responsible for these observed benefits remain largely unexplored.

Here, we tested the effect of systemically administered hASCs in immunodeficient mice treated with multiple low doses of streptozotocin (MLDS-STZ) with the goal of identifying key ASC-derived factors responsible for β cell specific beneficial effects. Human ASCs improved glucose homeostasis in STZ-treated mice through maintenance of β cell mass and increased β cell proliferation. *In vitro*, hASCs promoted human and mouse islet and INS-1 cell survival following prolonged culture and/or cytokine stress. To provide a mechanistic basis for these effects, factors liberated from hASCs in response to β cell stress were identified using multiplex assays and candidate-based approaches. Most notably, we have identified a novel role for tissue inhibitor of metalloproteinase 1 (TIMP-1) in ASC-mediated pro-survival effects.

RESEARCH DESIGN AND METHODS

Reagents

Human specific TIMP-1 and VEGF ELISAs were from Abcam (Cambridge, MA). Mouse and human IL-1β, IFN-γ and TNF-α were obtained from Invitrogen, (Carlsbad, CA). A function-blocking TIMP-1 antibody was obtained from AbD Serotec (Raleigh, NC). Recombinant human insulin was from Novo Nordisk (Bagsvaerd, Denmark), and recombinant active human TIMP-1 was from Millipore (Billerica, MA). D-Luciferin-K+ was from PerkinElmer (Waltham, MA), prepared in PBS to yield a final concentration of 20mg/ml (pH 7), and stored in individual light tight aliquots at −20 °C until use. Unless specified, all other chemicals were from Sigma-Aldrich (St. Louis, MO). Supplemental Table 1 contains a complete list of antibodies.

Animals and cell culture

Male immunodeficient NOD/SCID/gchain^{null} (NOD/SCID) mice were from a breeding colony established at the Indiana University (IU) School of Medicine Laboratory Animal Research Center and maintained by the IU *In Vivo* Therapeutic Core within the Simon Cancer Center [21]. Male C57BL6/J mice were obtained from the Jackson Laboratory (Bar Harbor, ME) at 8 weeks of age. Animals were maintained under protocols approved by the IU Institutional Animal Care and Use Committee, the U.S. Department of Agriculture's Animal Welfare Act (9 CFR Parts 1, 2, and 3), and the Guide for the Care and Use of Laboratory Animals [22]. Mice were kept in pathogen-free conditions under a standard light-dark cycle with *ad libitum* access to chow diet and water.

At 8 weeks of age, NOD/SCID mice were injected intraperitoneally with 45 mg/kg STZ or PBS daily for 4 days. Intraperitoneal glucose tolerance tests (IPGTT) were performed as previously described using 2 mg/kg body weight of glucose delivered intraperitoneally [23]. Blood glucose concentrations were determined using an AlphaTRAK glucometer (Abbott Laboratories, Abbott Park, IL). Serum insulin levels were measured using an ultrasensitive mouse-specific ELISA (Crystal Chem, Chicago, IL). Pancreatic islets were isolated by collagenase digestion as described previously [24]. Human islets from 3 male and 2 female cadaveric non-diabetic donors were obtained from the Integrated Islet Distribution Program and cultured as previously described [25]. The average age of islet donors was 45.8 ± 3.9 yr (S.E.M). The average body mass index (BMI) was 32.9 ± 5.3 kg/m^2.

Human ASCs from non-diabetic donors were isolated as previously described from subcutaneous adipose tissue obtained from liposuction procedures [26]. Monolayers of hASCs from 4 female donors were passaged when 60–80% confluent, and used between passages 2–4. The average donor age was 32.0 ± 3.2 yrs; the average donor BMI was 25.1 ± 3.8 kg/m^2. Human ASCs were harvested with trypsin and resuspended in EBM-2/5%FBS media (Lonza, Allendale, NJ), at a final concentration of 2×10^7 cell per ml. STZ-treated NOD/SCID mice were anesthetized with 2.5% isoflurane and 100 μl of cell suspension or PBS was injected intravenously through the tail vein.

For tracking experiments, hASCs were transduced with GFP-expressing lentivirus as previously described [14] or a pCMV-VSVG luciferase-expressing lentivirus in EBM-2/5% FBS overnight, cultured for an additional 2 days, and injected into STZ-treated NOD/SCID/gchain^{null} mice. DNA from lung, pancreas, and hASCs was isolated using the DNeasy™ blood and tissue kit (Qiagen, Hilden, Germany) according to the manufacturer's instruction. PCR was performed using human or mouse specific primers for TNF-α genomic DNA as previously described [27]. Injected hASCs were detected as a human specific band in lung and pancreata using primer pairs for human genomic TNF-α. Results were compared to those obtained using primers for the mouse genomic TNF-α sequence. Dynamic Bioluminescence Images (DBLI) were acquired using the Berthold NightOwl (Berthold Technologies, Oak Ridge, TN) outfitted with a 24W inductive header (Zoo Med Laboratories, San Luis Obispo, CA) and a custom anesthesia manifold. Prior to imaging, mice were shaved and depilitated with Nair (Church and Dwight, Princeton, NJ). Anesthetic induction was achieved with 2–4% isoflurane, and 150 mg/kg D-luciferin was administered. Mice were immediately transferred to the imager's heated stage (40±1°C), and imaged sequentially at 2 min intervals for 44 mins with image integration times of 120 sec/image. At the completion of the sequence, anatomical reference photos were acquired to permit generation of parametric image sets.

To provide visualization, segmentation, and time series quantification, DBLI and anatomical reference images were imported into the custom-developed software eLumenate® (Copywrite© 2010–2012, Paul R. Territo, Ph.D). Pseudo-colored parametric overlays of DBLI and anatomical reference images suitable for time series quantification were dynamically constructed for each animal, and regions of interest were segmented through time using the semi-automated Maximum Entropy region of interest (ROI) algorithm [28] and plugin in eLumenate®. The extracted time series were then analyzed for peak emission (Cmax) and time to peak emission (Tmax) with eLumenate's Peak Analysis plugin.

For co-culture experiments, mouse or human islets were placed on Millicell inserts with 1 μm pores (Millipore, Billerica, MA) with or without hASCs cultured at the bottom of 24-well plates. At indicated time points, islets were washed with PBS and stained using the Invitrogen Live/Dead Cell Viability Assay according to the manufacturer's instructions. Images were acquired on a Zeiss Z1 inverted microscope equipped with an Orca ER CCD camera (Hamamatsu Photonics, Hamamatsu City, Japan). Following dissociation into single cell suspension, by gentle pipetting in Ca^{2+}-free PBS supplemented with 0.025% trypsin/EDTA, the percentage of dead cells was calculated using a SpectraMax M5 microplate reader (Molecular Devices, Sunnyvale, CA).

Supernatants from mouse and hASC co-culture experiments were collected at 2, 4, and 6 days and subjected to multiplex analysis using the Bio-plex® Pro Human Cytokine 27-Plex Assay (Bio-Rad Laboratories, Hercules, CA). Results were complemented with candidate based ELISA screens based on existing literature

INS-1 cells (832/13) were cultured as previously described [25] and pretreated with TIMP-1 for 3h followed by treatment with IL-1β, IFN-γ and TNF-α for 48h.

β Cell Mass, immunohistochemistry and immunofluorescence analysis

Following euthanasia and intracardiac administration of 4% paraformaldehyde, pancreata and other selected tissues were rapidly dissected. β cell mass was calculated as previously described [29]. To assess proliferation, pancreatic sections from *in vivo* experiments were immunostained for insulin, phospho-histone H3 (PH3), and DAPI. Cells positive for both insulin and PH3 were determined to be PH3 positive β cells, and counted using Image J software. Staining for glucagon, insulin and DAPI in pancreatic sections was performed as previously described and stained cells were counted using Image J [30]. For tracking analyses, lung and pancreatic sections were immunostained for GFP and insulin. INS-1 cells were fixed in 4% paraformaldehyde and permeabilized with 0.05% Triton X-100 followed by immunostaining for PH3 or cleaved caspase-3.

Glucose-Stimulated Insulin Secretion

Approximately sixty human islets were co-cultured with ASCs, and glucose-stimulated insulin secretion (GSIS) was performed as previously described [31]. Insulin was assayed using the Coat-A-Count insulin solid-phase RIA (Siemens Medical Solutions, Malvern, PA). Insulin secretion was normalized to the total islet protein content.

Statistical analysis

Differences between groups were examined for significance with either the two-tailed Student's *t* test or one-way ANOVA followed by the Tukey-Kramer posttest using GraphPad Prism statistics software (GraphPad Software, Inc., San Diego, CA). A P value of <0.05 was taken to indicate the presence of a significant difference.

RESULTS

Systemic administration of hASCs improves glucose tolerance, islet morphology and β cell mass in STZ-treated NOD-SCID mice

To characterize the effects of hASCs on an *in vivo* model of hyperglycemia, NOD-SCID mice were treated with multiple low doses of STZ according to the timeline outlined in Fig 1A. Intraperitoneal glucose tolerance tests (IPGTTs) were performed on day 7 after the start of STZ administration (Fig. 1B). Two groups of STZ-treated mice were evaluated prior to cell or control carrier infusion to ensure identical degrees of glucose intolerance, and PBS or 2×10^6 hASCs were administered via tail vein injection. Repeat IPGTTs were performed 17–20 and 35 days after STZ administration (Fig. 1C–D). While both groups of STZ-treated mice exhibited significantly increased glucose excursions during IPGTT, hASC-treated mice demonstrated improved glucose tolerance compared to mice receiving STZ and PBS. At day

17–20, the glucose AUC was significantly lower in hASC-treated mice compared to mice that received STZ and PBS, and the effect was durable through day 35 (Fig. 1E). STZ-treated mice receiving hASCs also had significantly higher serum insulin levels after i.p. glucose injection compared to STZ-treated mice that received only PBS (Fig. 1F).

Both STZ-treated groups demonstrated a marked disruption in the expected murine islet architecture [32] and had decreased β cell mass compared to controls (Fig. 2A and F). However, compared to mice receiving STZ and PBS, STZ+hASC-treated mice demonstrated a significant preservation of insulin staining and β cell mass (STZ+hASC; 1.69 ± 0.18 mg vs STZ; 0.79 ± 0.08 mg) (Fig. 2A and E–F). We next determined changes in islet α and β cell number (Fig. 2B and F). Similar to β cell mass results, the average number of β cells per islet was decreased after STZ treatment with a tendency towards increased β cell number with hASC injection (control; 111.3 ± 31.6 cells/islet vs STZ; 29.3 ± 7.1 cells/islet vs STZ+hASC; 57.9 ± 7.2 cells/islet). In contrast, there was no significant change in α cell number across treatment groups.

β cell proliferation was assessed by co-staining pancreatic sections for insulin and PH3, which marks cells in the G2 and M phases of mitosis [33]. STZ+hASCs treated mice displayed a significantly higher number of PH3 positive β cells (double positive cells for PH3 and insulin) per islet compared to control and STZ-treated mice that received PBS (Fig. 2C and G). Moreover, STZ+hASC mice had a significantly higher percentage of PH3 positive β cells compared to controls that did not receive STZ (Fig. 2D and G).

Islet viability is improved by hASC co-culture

To investigate the ability of hASCs to support islet survival and function *in vitro*, C57BL6/J mouse islets exposed to hASC-conditioned media via a transwell system were stained using a live/dead assay after 6 days of co-culture. Fluorescent images demonstrated a decrease in red, ethidium homodimer-1 positive cells, indicative of decreased dead cells. A parallel increase in viable, calcein-AM positive green cells was noted in islets co-cultured with hASCs (Fig. 3A). Following islet dissociation, these results were quantified using a fluorescent plate reader, confirming that hASCs improved mouse islet survival following prolonged culture (Fig. 3B).

Characterization of the paracrine cross-talk between co-cultured islets and hASCs

Previous studies have shown that ASCs actively secrete of a number of cytokines and growth factors [34], and secretion of these factors appears to be a critical component of the therapeutic effects of ASCs in other disease models [15, 16]. In order to determine the specific hASC-derived factors secreted in response to aging and stressed islets, supernatants from hASC and C57BL6/J mouse islet co-culture experiments were collected at day 2, 4, and 6 of co-culture and subjected to multiplex or ELISA analysis of specific human-derived factors. A number of human growth factors including IL-6, IL-8, IL-12, eotoxin, IP10, MCP-1, VEGF, and TIMP-1 were identified in supernatants from co-culture experiments (Supplemental Fig. S1). Notably, secretion of a subset of these factors, including IP10, eotaxin, VEGF, and TIMP-1 was increased with islet co-culture, suggesting the presence of paracrine cross-talk between islets and hASCs (Fig. 3C–F). Interestingly, TIMP-1, which in

isolation has been shown to protect against cytokine and STZ-induced β cell death [35, 36], was found to be the most highly enriched factor in co-culture supernatants. In mouse islet/hASC co-cultures, human TIMP-1 levels were nearly 600-fold higher than VEGF, the second most enriched factor. Furthermore, TIMP-1 secretion from hASCs was increased approximately 1.5-fold in the presence of islets cultured *ex vivo* for 6 days. Complete results from the multiplex assay are shown in Supplemental Fig. S1.

Similar results were observed when human islets were co-cultured with hASCs. While this experimental design did not allow us to definitively assay whether TIMP-1 was solely released from the ASC fraction, secretion of TIMP-1 into the supernatant was significantly increased after 6 days of co-culture with cadaveric human islets (Fig. 3G).

In order to characterize TIMP-1 secretion patterns, independent of effects of islet co-culture, a time course analysis was performed using hASCs from 3 different human donors. Results demonstrated a rapid accumulation of TIMP-1 in the media, and levels continued to increase through 48h, at which point the concentration reached 1669 ± 273 ng/mg protein (Fig. 4A). ASC supernatants were subjected to western blot analysis for verification and similar results were noted (Fig. 4B). To determine what additional factors might lead to increased secretion of TIMP-1, hASCs were incubated directly with recombinant human insulin at concentrations of 1, 10, and 100 nM. No significant difference in TIMP-1 secretion was noted in the presence of insulin at any of the three tested concentrations (Fig. 4C).

Pro-inflammatory cytokines stimulate TIMP-1 secretion from hASCs and TIMP-1 blockade abrogates the pro-survival effects of hASCs

We next sought to determine whether TIMP-1 secretion would be increased in the presence of the pro-inflammatory milieu that typifies T1DM. Human ASCs were treated with a combination of 10 ng/mL TNF-α, 100 ng/mL IFN-γ, and 5 ng/mL IL-1β. Treatment with the cytokine mixture significantly increased TIMP-1 secretion from hASCs (Fig. 5A-B). To assess β cell insulin secretory function, human islets were placed in the co-culture system and treated with INF-γ, TNF-α, and IL-1β. The insulin secretory index was significantly increased in cytokine-treated islets co-cultured with hASCs compared to cytokine-treated islets cultured alone. (Fig. 5C).

We next tested whether TIMP-1 blockade would impact the ability of hASCs to support islet survival under T1DM conditions. Human islets and hASCs were co-cultured in a transwell system and treated with the combination of cytokines in the presence or absence of a TIMP-1 blocking antibody. Treatment with the cytokines increased expression of cleaved caspase-3, pJNK, and iNOS. Exposure to hASC-conditioned media significantly decreased cleaved caspase-3 activation within the islet fraction, while addition of the TIMP-1 blocking antibody partially blocked this pro-survival effect. In the presence of TIMP-1 blocking antibody, activation of cleaved caspase-3 was significantly increased compared to islets cultured with hASCs alone (Fig 5D-E). Similar trends were noted with pJNK and iNOS, but these results did not reach statistical significance.

Systemically administered hASCs can be detected at low levels in the pancreas following STZ injection

To determine the extent to which our *in vivo* results might be attributed to either local or systemic effects of hASCs, tracking experiments were performed. Human ASCs were transduced with GFP-expressing lentivirus and injected according to the schematic outlined in Fig. 6A. Lung tissue was stained for GFP as a positive control. GFP positive cells were readily detected in lung in both immunohistochemistry (Fig. 6B) and immunofluorescence analysis (Fig. 6C). GFP positive cells were also found in the pancreata of injected mice three days after tail vein delivery of hASCs. The cells were seen less frequently in the pancreas compared to the lung, but GFP-positive cells were noted in both intraislet and extraislet locations. Confirming these findings, PCR analysis demonstrated the presence of human specific genomic DNA in samples from lung and pancreas of hASC-injected mice (Fig. 6D–E). Although it did not reach statistical significance, the average human DNA ratio in lung was about 12.9-fold higher than that of pancreas ($p=0.0531$). Fig. 6F confirms that PCR primers for human and mouse DNA showed similar efficiency of amplification (slope of the curve were −3.51 vs −3.53).

As a second quantitative approach, bioluminescent imaging was performed 1 day after luciferase-expressing hASCs were administered to STZ-treated or untreated NOD-SCID mice. A strong signal was detected bilaterally in the lung region as would be expected from a tail vein injection strategy. A lower imaging signal was detected in the abdomen, which included the region of the pancreas (Fig. 6GH).

To determine if there were additional systemic effects of hASCs, human TIMP-1 was measured in the serum following stem cell injection. Human TIMP-1 was undetectable in the serum of control NOD-SCID mice not injected with hASCs. However, serum human TIMP-1 levels rose to 20 ng/mL in STZ-treated mice who had received hASCs via tail vein injection (Fig. 6I). Of note, human VEGF could not be detected in the serum (data not shown).

Finally, to demonstrate specific effects of TIMP-1, INS-1 832/13 β cells were treated with INF-γ, TNF-α, and IL-1β in the presence or absence of the human recombinant TIMP-1. Cytokine treatment significantly reduced the number of PH3 positive INS-1 cells and increased the number of cleaved caspase-3 positive INS-1 cells. TIMP-1 treatment did not impact the percentage of PH3 positive cells. In contrast, the percentage of cleaved caspase-3 positive INS-1 β cells was significantly decreased by TIMP-1 treatment.

DISCUSSION

Stem cells derived from the stromal vascular fraction of adipose tissue have been shown to harbor significant potential for tissue repair in wide variety of disease models including myocardial infarction, wound healing, emphysema, hindlimb ischemia, and hypoxia-induced neuronal damage [14–18]. A recent report also demonstrated an ability of mouse ASCs to prevent hyperglycemia and β cell death in diabetic NOD mice, an effect that was attributed to attenuation of the TH1 immune response and expansion of regulatory T cells [20]. Likewise, several groups have reported improved outcomes in pre-clinical models of islet

transplantation following co-transplantation of islets combined with mouse ASCs. Analysis of these hybrid grafts showed enhanced graft revascularization, a finding consistent with the known role of ASCs to function as pericytes to support the growth of new blood vessels [19, 26]. To date, however, the specific ASC-derived factors responsible for their tissue repair and pro-survival effects, , in the context of the islet β cell have remained largely unexplored.

We tested the effect of systemically administered human ASCs in streptozotocin-induced diabetes in NOD-SCID mice. As anticipated, hASCs improved glucose homeostasis in STZ-treated mice, preserved β cell mass, and increased β cell proliferation. Data from *in vivo* experiments were consistent with an hASCs to improve β cell survival and enhance regeneration of the β cell pool, without any impact on the islet α cell compartment. *In vitro* co-culture experiments using mouse islets and hASCs in a transwell system were performed to query specific ASC-derived factors released in response to β cell stress, resulting from either prolonged culture or pro-inflammatory cytokine treatment. Our studies revealed that several secreted factors were involved in the paracrine network established between ASCs and islets. In particular, we have identified a potentially novel role for TIMP-1 as a highly enriched hASC-derived factor that promotes β cell survival under inflammatory conditions.

TIMP-1 is a member of the matrix metalloproteinase inhibitor (MMP) family and is recognized to regulate a variety of biological processes including cell growth, migration, and apoptosis. TIMP-1 has important MMP-dependent and independent actions. In other cell types, TIMP-1's MMP-independent effects to promote growth and inhibit apoptosis occur through activation of several different signaling pathways including P13K and PKA [37]. A limited number of studies have investigated the pro-survival effects of TIMP-1 in the β cell. A recent study showed that TNF-related apoptosis-inducing ligand (TRAIL) overexpression was able to decrease diabetes in NOD mice, and these effects occurred in parallel with increased TIMP-1 expression in islets [38]. Han *et al*. showed that TIMP-1 but not TIMP-2 was able to prevent cytokine-induced death and dysfunction in INS-1 cells, and TIMP-1 was found to reduce NF-kB activation in the presence of cytokines [36]. Notably, TIMP-1 overexpressing mice were also protected against STZ-induced diabetes. Following treatment with STZ at a dose of 40mg/kg/day for 5 days, TIMP-1 overexpressing mice had improved glucose homeostasis and preserved β cell mass. In agreement with our results, islets from these mice also exhibited increased β cell regeneration post-STZ [35].

Together, these data suggest an important role for TIMP-1 in β cell survival under inflammatory conditions. However, few studies have examined the specific role of TIMP-1 in ASC-mediated reparative effects. Our data show that hASCs from multiple donors robustly produced and secreted TIMP-1, and *in vitro* data show that TIMP-1 blockade with a neutralizing antibody reduced ASC-mediated β cell survival following treatment with a cocktail of pro-inflammatory cytokines that included TNF-α, IFN-γ, and IL-1β. In addition, our data also demonstrate a direct effect of recombinant TIMP-1 to decrease INS-1 β cell death induced by this same combination of pro-inflammatory cytokines.

We acknowledge that it is unlikely that only one ASC-derived factor is solely responsible for our observed results. TIMP-1 blocking antibody only partially impacted activation of cleaved caspase-3, while direct incubation of INS-1 cells with TIMP-1 was unable to restore

cytokine-induced reduction in proliferation. These results indicate a likely effect of other ASC-derived factors to promote β cell survival as well as regeneration/proliferation post-STZ. *In vitro* experiments revealed that ACSs also secreted high levels of VEGF, which is a potent pro-angiogenic factor in the islet. STZ is known to affect the integrity of islet microvasculature, and endogenous β cell regeneration from STZ also likely depends on recovery of this vasculature structure [39, 40]. Therefore, it is probable that ASC-derived VEGF aided outcomes in our study. In contrast to TIMP-1, we did not detect systemic elevations of VEGF, but this does not rule out the possibility that local intraislet levels were increased.

Interestingly, the pro-survival effects of hASCs observed in our study were seen in the context of a transwell system that was specifically selected to bypass cell-to-cell contact. This differs from both the Bassi *et al*. study and previous co-transplantation studies where immunomodulatory and pro-angiogenic effects of mouse ASCs were dependent on the direct contact of ASCs with immune cells or islets [19, 20]. While our tracking experiments demonstrated the presence of hASCs within the pancreas and islet, our results also showed enrichment of human TIMP-1 in the circulation of ASC-injected mice, suggesting benefits were likely derived from a combination of locally as well systemic effects.

Human ASC secretion of TIMP-1 as well as VEGF was potentiated in models where islets were stressed by either prolonged *ex vivo* culture or pro-inflammatory cytokines. The potential for cross-talk between adult stem cells and potential target tissues is important to consider as the field of regenerative medicine and regulatory agencies decide whether cell-based or factor-based strategies should be advanced. Our data demonstrates a dynamic interaction between the hASCs and stressed islets that ultimately impacted behavior of the hASCs. This same interaction may be difficult to recapitulate if only static, factor-based approaches are employed.

Both mouse and human adipose derived stromal cells have been exposed to *in vitro* differentiation strategies aimed at generating insulin-positive cells. Upon transplantation into diabetic mice, these insulin-producing cells have shown varying abilities to reverse STZ-induced hyperglycemia in rodent models [41, 42]. Recent case reports have also tested similar strategies in humans with modest improvements in glycemic control and insulin secretion [43]. Directed differentiation of ASCs may occur in an *in vitro* context, however it seems a less likely contributor to the results observed in our study given the number of hASCs observed in the pancreas. Finally, our study focused on the effects of hASCs on β cell survival and function. While STZ is primarily a β cell toxin, previous studies suggest that STZ treatment may also induce a mild component of peripheral insulin resistance [44], and we cannot rule out the possibility that hASCs also affected this parameter.

Several additional issues bear resolving prior to the implementation of ASCs as a potential clinical treatment for human diabetes. First, little is known about the effects of repeated passaging on ASC identity. Long-term culture has been shown to affect several aspects of ASC biology including their proliferative and trophic capacity [45, 46]. Variations related to donor differences are also important to understand. If cells are to be employed in an autologous fashion in diabetic individuals, then studies are needed to understand how

diabetes *per se* affects the pro-survival and regenerative properties of ASCs. A key translational aspect of our study is that it was performed using human ASCs from 4 different donors. However, these individuals were young and non-diabetic with an average BMI of 25.1. While our results suggest that cytokines are capable of upregulating TIMP-1, a study by Cramer et al. demonstrated that elevated glucose enhanced senescence and apoptosis in hASCs [47]. From a safety perspective, however, ASCs appear to have low intrinsic ability for teratoma formation [48]. Still, resolution of the aforementioned concerns should remain a priority, especially given the growing frequency of stem cell tourism where offshore companies provide infusion of autologous ASCs for a variety of conditions without consistent testing of safety or efficacy [49].

In conclusion, our results demonstrate that systemic administration of hASCs protects against STZ-induced hyperglycemia and loss of β cell mass. Notably, our studies describe a novel role for ASC-derived TIMP-1 in promoting β cell survival under *in vitro* pro-inflammatory conditions. Future studies are needed to determine the precise molecular pathways responsible for the beneficial effects of hASCs observed *in vivo* and to uncover whether there are donor-related differences in the ability of ASCs to support β cell survival in Type 1 diabetes mellitus.

Supplementary Material

Refer to Web version on PubMed Central for supplementary material.

Acknowledgments

This work was supported by NIH grants T32 HL079995 (to T.M.K.), T32 DK065549 (to E.K.S.), and K08 DK080225, R03 DK089147, and R01 DK093954 (to C.E.M.), and R01 CA138237-01 and R01 CA155294-01 (to H.H.), VA Merit Award 1I01BX001733 (to C.E.M.) and gifts from the R.B. Annis Educational Foundation (to C.E.M. and K.L.M.), Sigma Beta Sorority (to C.E.M.), and the Cryptic Masons' Medical Research Foundation (to K.L.M.). The funders had no role in study design, data collection and analysis, decision to publish, or preparation of the manuscript. The authors would like to thank George L. Vestermark, Young-sook Kim, and Stephanie Merfeld-Clauss for their expert technical assistance. Indiana University is a Center for Excellence in Molecular Hematology (P30)

ABBREVIATIONS

GSIS	Glucose stimulated insulin secretion
hASCs	Human adipose stromal/stem cells
IFN-γ	Interferon-gamma
IL-1β	Interleukin-1beta
MSCs	Mesenchymal stem cells
NOD/SCID/gchain^{null}	Non-Obese Diabetic/Severe Combined Immunodeficient/ interleukin 2 receptor gamma null
PH3	Phosphohistone H3
TIMP-1	Tissue Inhibitor of Matrix Metalloproteinase 1

TNF-α	Tumor necrosis factor alpha
VEGF	Vascular Endothelial Growth Factor

References

1. Tao B, Pietropaolo M, Atkinson M, et al. Estimating the cost of type 1 diabetes in the U.S.: a propensity score matching method. PLoS One. 2010; 5:e11501. [PubMed: 20634976]
2. Control CfD. [Accessed 01/01/2013, 2013.] National Health Interview Survey. Available at: www.cdc.gov
3. Imperatore G, Boyle JP, Thompson TJ, et al. Projections of Type 1 and Type 2 Diabetes Burden in the U.S. Population Aged <20 Years Through 2050: Dynamic modeling of incidence, mortality, and population growth. Diabetes Care. 2012; 35:2515–2520. [PubMed: 23173134]
4. Patterson CC, Dahlquist GG, Gyurus E, et al. Incidence trends for childhood type 1 diabetes in Europe during 1989–2003 and predicted new cases 2005–20: a multicentre prospective registration study. Lancet. 2009; 373:2027–2033. [PubMed: 19481249]
5. Stanescu DE, Lord K, Lipman TH. The epidemiology of type 1 diabetes in children. Endocrinol Metab Clin North Am. 2012; 41:679–694. [PubMed: 23099264]
6. Wajchenberg BL, Feitosa AC, Rassi N, et al. Glycemia and cardiovascular disease in type 1 diabetes mellitus. Endocr Pract. 2008; 14:912–923. [PubMed: 18996824]
7. Trence DL, Hirsch IB. Motherhood, apple pie, hemoglobin A(1C), and the DCCT. Endocr Pract. 2012; 18:78–84. [PubMed: 22336443]
8. Barton FB, Rickels MR, Alejandro R, et al. Improvement in outcomes of clinical islet transplantation: 1999–2010. Diabetes Care. 2012; 35:1436–1445. [PubMed: 22723582]
9. Gruessner AC, Sutherland DE, Gruessner RW. Long-term outcome after pancreas transplantation. Curr Opin Organ Transplant. 2012; 17:100–105. [PubMed: 22186094]
10. Xie R, Everett LJ, Lim HW, et al. Dynamic Chromatin Remodeling Mediated by Polycomb Proteins Orchestrates Pancreatic Differentiation of Human Embryonic Stem Cells. Cell Stem Cell. 2013
11. Lee RH, Seo MJ, Reger RL, et al. Multipotent stromal cells from human marrow home to and promote repair of pancreatic islets and renal glomeruli in diabetic NOD/scid mice. Proc Natl Acad Sci U S A. 2006; 103:17438–17443. [PubMed: 17088535]
12. Ezquer F, Ezquer M, Contador D, et al. The antidiabetic effect of mesenchymal stem cells is unrelated to their transdifferentiation potential but to their capability to restore Th1/Th2 balance and to modify the pancreatic microenvironment. Stem Cells. 2012; 30:1664–1674. [PubMed: 22644660]
13. Bell GI, Putman DM, Hughes-Large JM, et al. Intrapancreatic delivery of human umbilical cord blood aldehyde dehydrogenase-producing cells promotes islet regeneration. Diabetologia. 2012; 55:1755–1760. [PubMed: 22434536]
14. Schweitzer KS, Johnstone BH, Garrison J, et al. Adipose stem cell treatment in mice attenuates lung and systemic injury induced by cigarette smoking. Am J Respir Crit Care Med. 2011; 183:215–225. [PubMed: 20709815]
15. Cai L, Johnstone BH, Cook TG, et al. Suppression of hepatocyte growth factor production impairs the ability of adipose-derived stem cells to promote ischemic tissue revascularization. Stem Cells. 2007; 25:3234–3243. [PubMed: 17901400]
16. Wei X, Zhao L, Zhong J, et al. Adipose stromal cells-secreted neuroprotective media against neuronal apoptosis. Neurosci Lett. 2009; 462:76–79. [PubMed: 19549558]
17. Hadad I, Johnstone BH, Brabham JG, et al. Development of a porcine delayed wound-healing model and its use in testing a novel cell-based therapy. Int J Radiat Oncol Biol Phys. 2010; 78:888–896. [PubMed: 20708345]
18. Hong SJ, Traktuev DO, March KL. Therapeutic potential of adipose-derived stem cells in vascular growth and tissue repair. Curr Opin Organ Transplant. 2010; 15:86–91. [PubMed: 19949335]

19. Fumimoto Y, Matsuyama A, Komoda H, et al. Creation of a rich subcutaneous vascular network with implanted adipose tissue-derived stromal cells and adipose tissue enhances subcutaneous grafting of islets in diabetic mice. Tissue Eng Part C Methods. 2009; 15:437–444. [PubMed: 19320553]
20. Bassi EJ, Moraes-Vieira PM, Moreira-Sa CS, et al. Immune regulatory properties of allogeneic adipose-derived mesenchymal stem cells in the treatment of experimental autoimmune diabetes. Diabetes. 2012; 61:2534–2545. [PubMed: 22688334]
21. Cai S, Wang H, Bailey B, et al. Humanized bone marrow mouse model as a preclinical tool to assess therapy-mediated hematotoxicity. Clin Cancer Res. 2011; 17:2195–2206. [PubMed: 21487065]
22. Animals CFTUOTGFTCAUOL. Guide for the Care and Use of Laboratory Animals. Washington (DC): National Academies Press; 2011.
23. Evans-Molina C, Robbins RD, Kono T, et al. Peroxisome proliferator-activated receptor gamma activation restores islet function in diabetic mice through reduction of endoplasmic reticulum stress and maintenance of euchromatin structure. Mol Cell Biol. 2009; 29:2053–2067. [PubMed: 19237535]
24. Stull ND, Breite A, McCarthy R, et al. Mouse islet of Langerhans isolation using a combination of purified collagenase and neutral protease. J Vis Exp. 2012
25. Kono T, Ahn G, Moss DR, et al. PPAR-gamma activation restores pancreatic islet SERCA2 levels and prevents beta-cell dysfunction under conditions of hyperglycemic and cytokine stress. Mol Endocrinol. 2012; 26:257–271. [PubMed: 22240811]
26. Traktuev DO, Prater DN, Merfeld-Clauss S, et al. Robust functional vascular network formation in vivo by cooperation of adipose progenitor and endothelial cells. Circ Res. 2009; 104:1410–1420. [PubMed: 19443841]
27. Nitsche A, Becker M, Junghahn I, et al. Quantification of human cells in NOD/SCID mice by duplex real-time polymerase-chain reaction. Haematologica. 2001; 86:693–699. [PubMed: 11454523]
28. Sin, CF.; Leung, CK. Image segmentation by edge pixel classification with maximum entropy. From the International Symposium on Intelligent Multimedia, Video, and Speech Processing. IEEE Conference Publications; 2001.
29. Maier B, Ogihara T, Trace AP, et al. The unique hypusine modification of eIF5A promotes islet beta cell inflammation and dysfunction in mice. J Clin Invest. 2010; 120:2156–2170. [PubMed: 20501948]
30. Sims EK, Hatanaka M, Morris DL, et al. Divergent compensatory responses to high-fat diet between C57BL6/J and C57BLKS/J inbred mouse strains. Am J Physiol Endocrinol Metab. 2013; 305:E1495–1511. [PubMed: 24169046]
31. Ogihara T, Chuang JC, Vestermark GL, et al. Liver X receptor agonists augment human islet function through activation of anaplerotic pathways and glycerolipid/free fatty acid cycling. J Biol Chem. 2010; 285:5392–5404. [PubMed: 20007976]
32. Levetan CS, Pierce SM. Distinctions Between the Islets of Mice and Men: Implications for New Therapies for Type 1 and 2 Diabetes. Endocr Pract. 2012:1–36.
33. Wei Y, Mizzen CA, Cook RG, et al. Phosphorylation of histone H3 at serine 10 is correlated with chromosome condensation during mitosis and meiosis in Tetrahymena. Proc Natl Acad Sci U S A. 1998; 95:7480–7484. [PubMed: 9636175]
34. Lee MJ, Kim J, Kim MY, et al. Proteomic analysis of tumor necrosis factor-alpha-induced secretome of human adipose tissue-derived mesenchymal stem cells. J Proteome Res. 2010; 9:1754–1762. [PubMed: 20184379]
35. Jiang H, Zhu H, Chen X, et al. TIMP-1 transgenic mice recover from diabetes induced by multiple low-dose streptozotocin. Diabetes. 2007; 56:49–56. [PubMed: 17192464]
36. Han X, Sun Y, Scott S, et al. Tissue inhibitor of metalloproteinase-1 prevents cytokine-mediated dysfunction and cytotoxicity in pancreatic islets and beta-cells. Diabetes. 2001; 50:1047–1055. [PubMed: 11334407]
37. Stetler-Stevenson WG. Tissue inhibitors of metalloproteinases in cell signaling: metalloproteinase-independent biological activities. Sci Signal. 2008; 1:re6. [PubMed: 18612141]

38. Kang S, Park EJ, Joe Y, et al. Systemic delivery of TNF-related apoptosis-inducing ligand (TRAIL) elevates levels of tissue inhibitor of metalloproteinase-1 (TIMP-1) and prevents type 1 diabetes in nonobese diabetic mice. Endocrinology. 2010; 151:5638–5646. [PubMed: 21047948]
39. Papaccio G, Chieffi-Baccari G. Alterations of islet microvasculature in mice treated with low-dose streptozocin. Histochemistry. 1992; 97:371–374. [PubMed: 1535618]
40. Watada H. Role of VEGF-A in pancreatic beta cells. Endocr J. 2010; 57:185–191. [PubMed: 20179357]
41. Zhang S, Dai H, Wan N, et al. Promoting long-term survival of insulin-producing cell grafts that differentiate from adipose tissue-derived stem cells to cure type 1 diabetes. PLoS One. 2011; 6:e29706. [PubMed: 22216347]
42. Chandra V, Swetha G, Muthyala S, et al. Islet-like cell aggregates generated from human adipose tissue derived stem cells ameliorate experimental diabetes in mice. PLoS One. 2011; 6:e20615. [PubMed: 21687731]
43. Dave SD, Trivedi HL, Chooramani SG, et al. Management of type 1 diabetes mellitus using in vitro autologous adipose tissue trans-differentiated insulin-making cells. BMJ Case Rep. 2013:2013.
44. Blondel O, Bailbe D, Portha B. In vivo insulin resistance in streptozotocin-diabetic rats--evidence for reversal following oral vanadate treatment. Diabetologia. 1989; 32:185–190. [PubMed: 2666209]
45. Safwani WK, Makpol S, Sathapan S, et al. The impact of long-term in vitro expansion on the senescence-associated markers of human adipose-derived stem cells. Appl Biochem Biotechnol. 2012; 166:2101–2113. [PubMed: 22391697]
46. Wan Safwani WK, Makpol S, Sathapan S, et al. The changes of stemness biomarkers expression in human adipose-derived stem cells during long-term manipulation. Biotechnol Appl Biochem. 2011; 58:261–270. [PubMed: 21838801]
47. Cramer C, Freisinger E, Jones RK, et al. Persistent high glucose concentrations alter the regenerative potential of mesenchymal stem cells. Stem Cells Dev. 2010; 19:1875–1884. [PubMed: 20380516]
48. MacIsaac ZM, Shang H, Agrawal H, et al. Long-term in-vivo tumorigenic assessment of human culture-expanded adipose stromal/stem cells. Exp Cell Res. 2012; 318:416–423. [PubMed: 22185824]
49. Levine AD, Wolf LE. The roles and responsibilities of physicians in patients' decisions about unproven stem cell therapies. J Law Med Ethics. 2012; 40:122–134. [PubMed: 22458467]

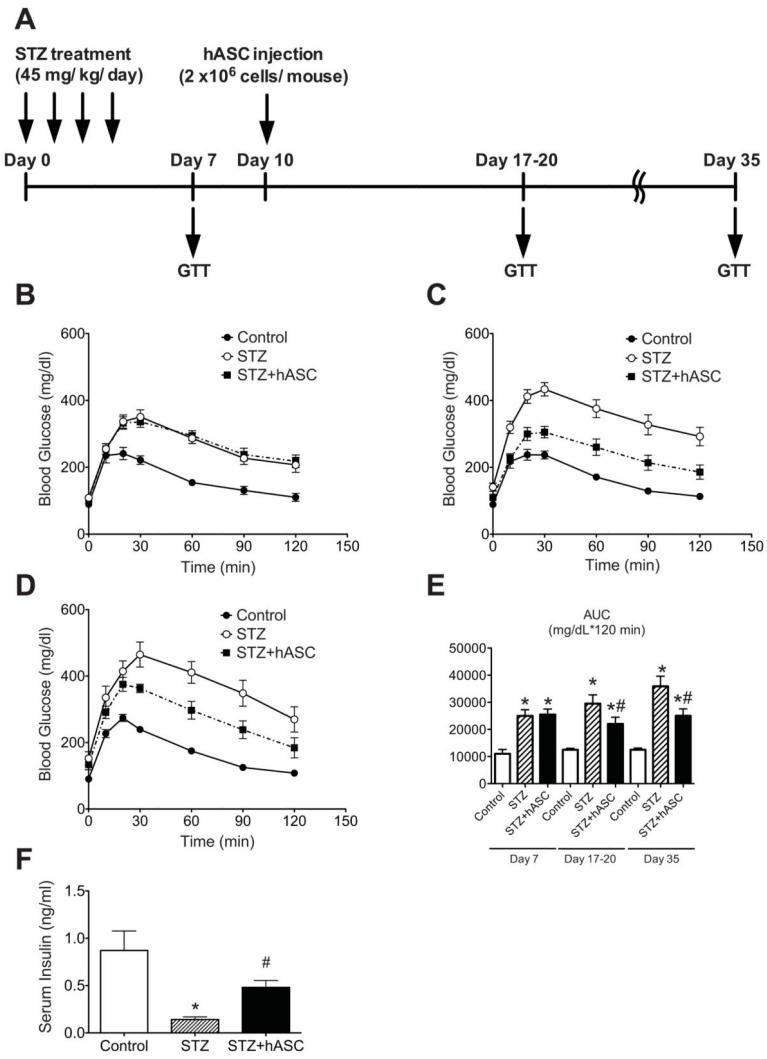

Figure 1. Systemic administration of hASCs improves glucose tolerance in STZ-treated NOD/SCID mice

A: Timeline for STZ and hASC injection and metabolic analyses. STZ (45 mg/kg/day) was administered daily for 4 days. IPGTT was performed on day 7 to document equal degrees of glucose intolerance in treatment groups, and PBS or 2×10^6 hASCs were injected via the tail vein. Repeat IPGTTs were performed 17–20 and 35 days after initial STZ injection. B–D: Results of IPGTTs performed on treated mice (STZ-un-injected controls (Control) = ●, Mice that received STZ with tail vein injection of only PBS (STZ) = ○, Mice that received STZ and tail vein injection of hASCs (STZ+hASCs) = ■) on day 7 (B) and day 17–20 (C); n=10–19 per group. D: IPGTT was repeated on day 35; n=5–6 per group. E: Area under curve (AUC) analyses for glucose excursion above baseline during IPGTTs. F: Serum insulin concentration 30 min after i.p. glucose injection on day 17; n=5 mice per group. Results are expressed as the means ± S.E.M.*$p<0.05$ compared to Control; $^{\#}p<0.05$ compared to STZ-treated mice.

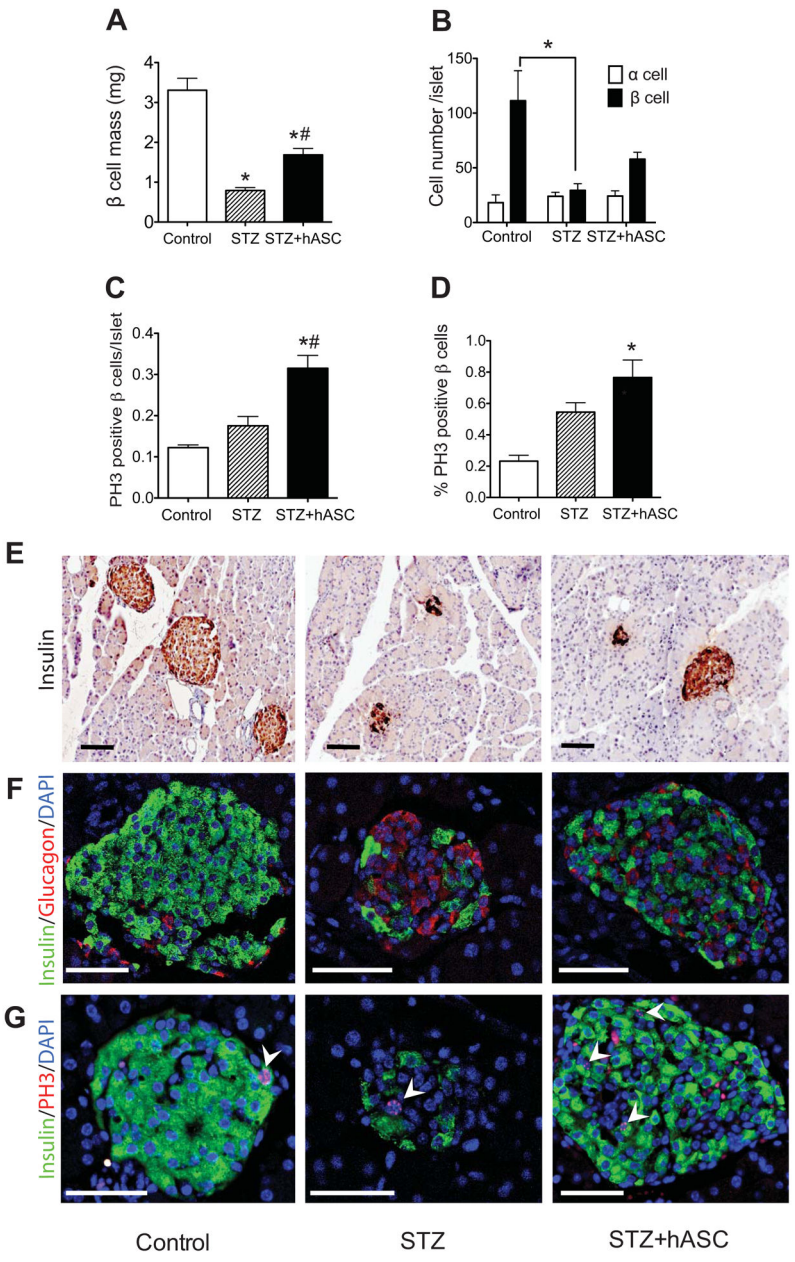

Figure 2. Systemic administration of hASCs improves islet morphology and β cell mass in STZ-treated NOD-SCID mice

A: Average β cell mass in PBS-treated controls, STZ-treated, and STZ+hASC-treated mice. B: Average cell number of glucagon positive cell (α cells) and insulin positive cells (β cells) per islet at day 17. C–D: PH3 was used to detect proliferating β cells. C: Number of PH3 positive β cells per islet. D: Percentage of PH3 positive β cells. Results are expressed as the means ± S.E.M; n=4 mice per group. *$p<0.05$ compared to Control; $^{\#}p<0.05$ compared to STZ-treated mice. E–G: Representative images of pancreata from indicated treatment group 7 days after hASC administration. Scale bars = 100 μm. E: Insulin immunocytochemistry shown at 20X magnification. F: Immunofluorescent detection of insulin (green) and glucagon (red) in islets of treated mice (40X magnification). G: Immunofluorescent

detection of insulin (green) and PH3 (red) shown at 40X magnification. Arrows depict cells double positive for insulin and PH3.

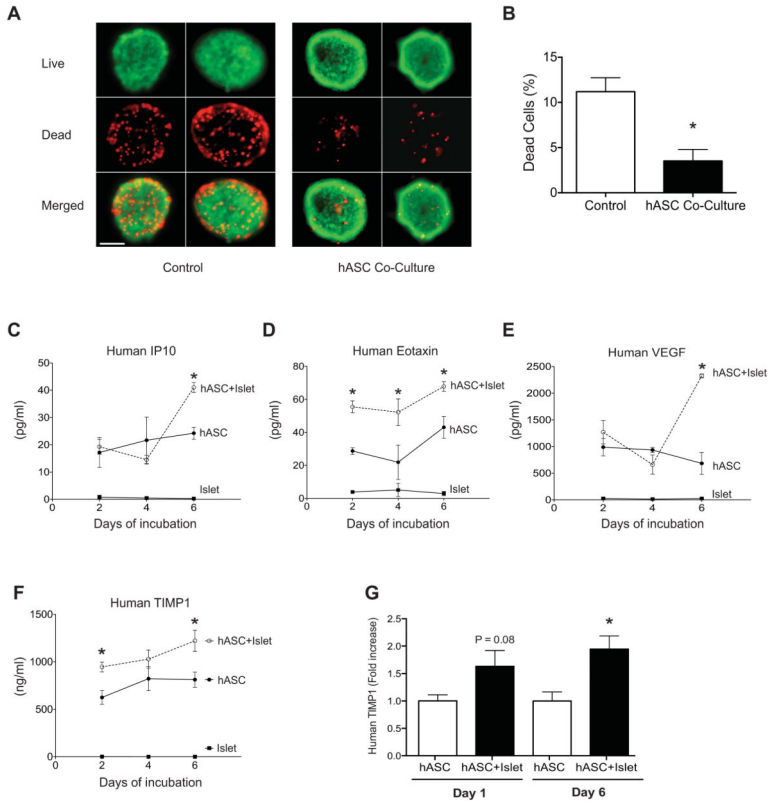

Figure 3. Co-culture with human ASCs improves islet viability, while human ASCs co-cultured with islets secrete TIMP-1 in excess of other paracrine factors

A: Live dead staining of C57BL6/J mouse islets co-cultured with (hASC Co-Culture) or without (Control) hASCs in a transwell system for six days. Representative fluorescent images of dead, ethidium homodimer-1 positive cells (red) and viable, calcein-AM positive cells (green) are shown at 20X magnification (scale bar = 50 μM). B: Quantification of the percentage of dead cells in dispersed islets cultured alone or with hASCs. *p<0.05 compared to islets cultured without hASCs. Results are expressed as the means ± S.E.M, n=3 independent experiments. C–F: ELISA and multiplex analysis of factors secreted by hASCs after 2, 4, and 6 days of islet co-culture. Supernatant concentration of human IP10 (C), human eotaxin (D), human VEGF (E), and human TIMP-1 (F). hASC alone = ●, hASC +C57BL6/J islets = ○, mouse islets alone = ■. Note, concentration of assayed factors is expressed as pg/mL except for TIMP-1, which is expressed as ng/ml. G: hASCs and human islets were co-cultured for 6 days in a transwell system. Supernatant concentration of human TIMP-1 was measured at day 1 and 6. *p<0.05 compared to hASCs cultured alone. Results are expressed as the means ± S.E.M. n=4 per group.

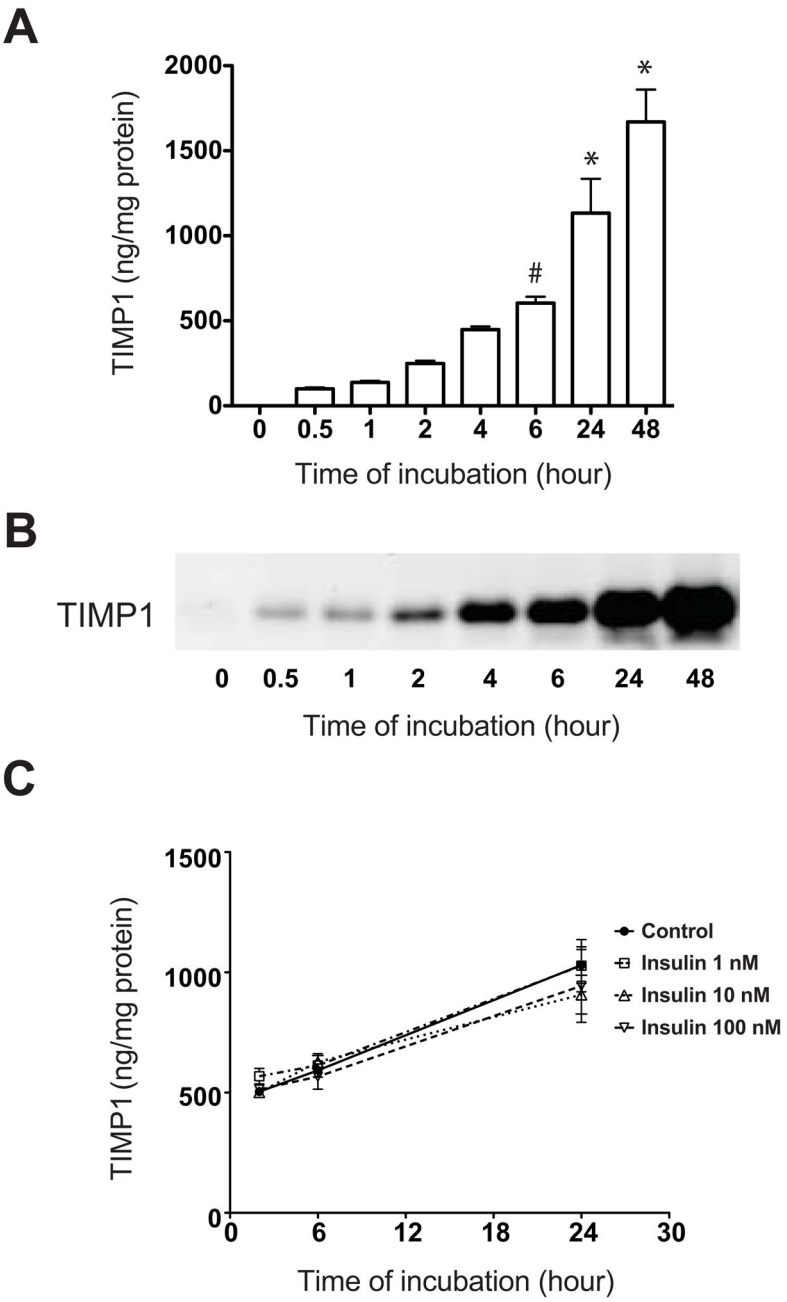

Figure 4. TIMP-1 secretion from hASCs is not altered by insulin

TIMP-1 secretion from cultured hASCs was measured by ELISA (A) and immunoblot (B). #p<0.05 compared to 0, 0.5 and 1 h; *p<0.05 compared to time 0, 0.5, 1, 2, 4 and 6 h. C: hASCs were cultured with human recombinant insulin (● = 0 nM, □ = 1 nM, △ = 10 nM, ▽ = 100 nM), and TIMP-1 secretion was measured by ELISA and normalized to total hASC protein. Results are expressed as the means ± S.E.M, where n=3 independent experiments.

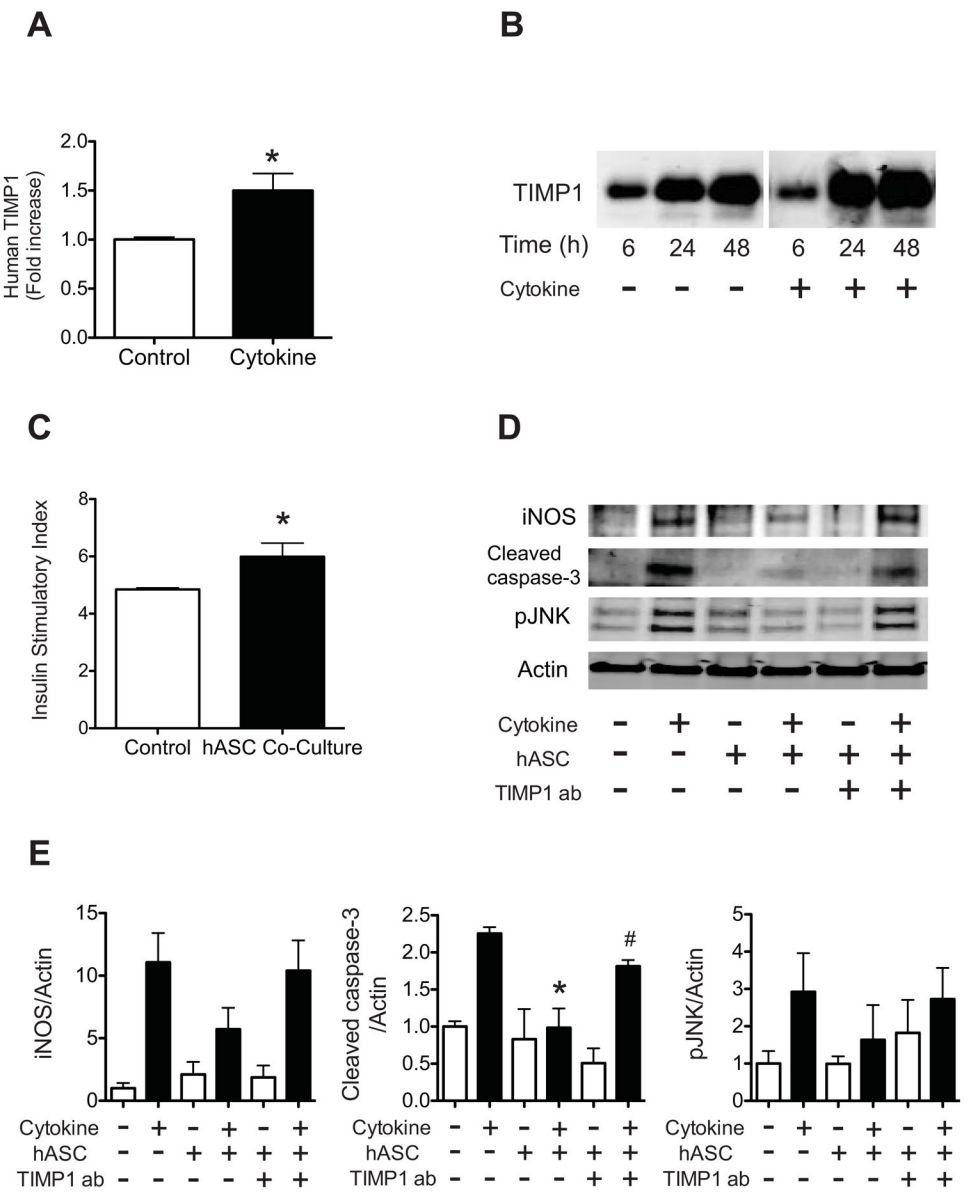

Figure 5. Pro-inflammatory cytokines stimulate TIMP-1 secretion from hASCs, while TIMP-1 neutralization abrogates the pro-survival effects of hASCs

A–B: hASCs were treated without (Control) or with 10 ng/mL TNF-α, 100 ng/mL IFN-γ, and 5 ng/mL IL-1β (Cytokine) for 24 hrs. A: TIMP-1 secretion was measured by ELISA and normalized to total protein. Results are expressed as the fold-increase compared to control. *p<0.05 compared to control treatment. B: Immunoblot of secreted TIMP-1 protein from hASCs treated with or without cytokines for indicated times. C: Human islets were co-cultured with (hASC Co-Culture) or without hASCs (Control) for 48 hrs followed by treatment with TNF-α, IFN-γ, and IL-1β for 6hrs. Glucose stimulated insulin secretion was performed as described in Material and Methods. Results are expressed as the ratio of insulin secreted under high glucose conditions compared to insulin secretion under low glucose conditions. *p<0.05 compared to cytokine-treated islets cultured alone. D–E:

Human islets were co-cultured with or without hASCs for 48 hrs combined with either normal rabbit IgG or TIMP-1 neutralizing antibody followed by 24hrs of treatment with TNF-α, IFN-γ, and IL-1β. D: Immunoblots for iNOS, cleaved caspase-3, and phosphorylated JNK. Actin was used as a loading control. Results are representative of four independent experiments. E: Quantification of protein levels in each treatment group from four independent experiments. *$p<0.05$ compared to cytokine treatment without hASCs or TIMP-1 blocking antibody; $^{\#}p<0.05$ compared to cytokine-treated islets co-cultured with hASCs and without TIMP-1 blocking antibody.

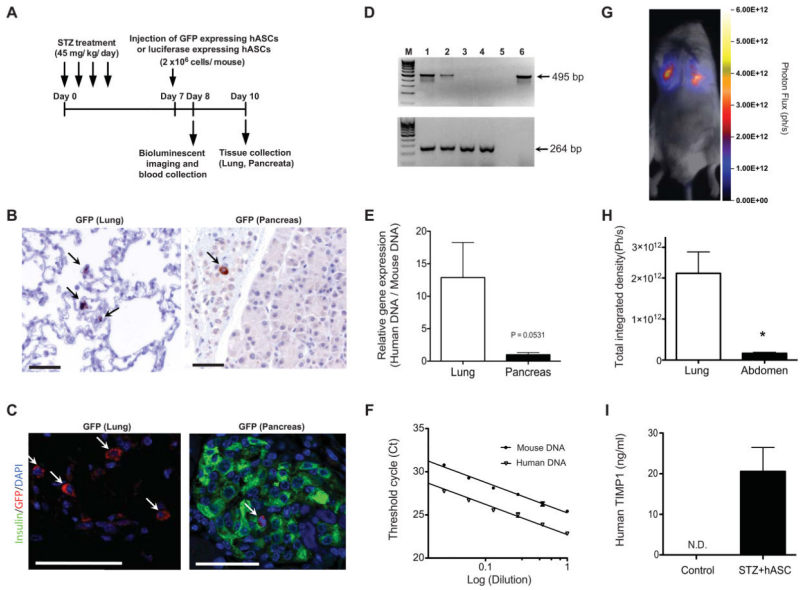

Figure 6. Systemically administered hASCs can be detected at low levels in the pancreas following STZ injection

A: Timeline for homing analysis. STZ (45 mg/kg/day) was administered daily for 4 days, and 2×10^6 GFP or luciferase expressing hASCs were injected via tail vein on day 7. Bioluminescent imaging and serum collection were performed on day 8. Tissues were collected for immunocytochemistry and immunofluorescent analysis on day 10. B–C: GFP immunocytochemistry of lung and pancreatic sections (B, 20X magnification), and immunofluorescence analysis of GFP (C, 40X magnification). Arrows indicate GFP positive cells. Scale bars = 50μm. D: Species-specific amplification of genomic DNA for hASC detection in lung and pancreata demonstrating different sizes for the human (495 bp; upper panel) and mouse (264 bp; lower panel) amplicons after 40 cycles. Lane M, marker; lane 1, lung from hASC-injected mouse; lane 2, pancreas from hASC-injected mouse; lane 3, lung from PBS-injected control mouse; lane 4, pancreas from PBS-injected control mouse; lane 5, PCR with no template (negative control); lane 6, hASCs (positive control for human gene). E: Real-time quantitative PCR for species-specific expression of genomic DNA. F: PCR efficiency curve for mouse and human primer sets. G: Bioluminescent *in vivo* whole-animal images were acquired from NOD/SCID mice treated with STZ+hASCs. Images were acquired one day after hASC administration. H: Quantification of total integrated density of luciferase labeled hASCs in lung and abdomen on day 8. *$p<0.05$ compared to lung. I: Serum TIMP-1 was measured using a human specific ELISA in STZ+hASC treated NOD/SCID mice and compared to NOD/SCID controls that did not receive hASC injection. N.D.= not detected. Results are expressed as the means ± S.E.M, n=at least 3 biological replicates for each experiment.

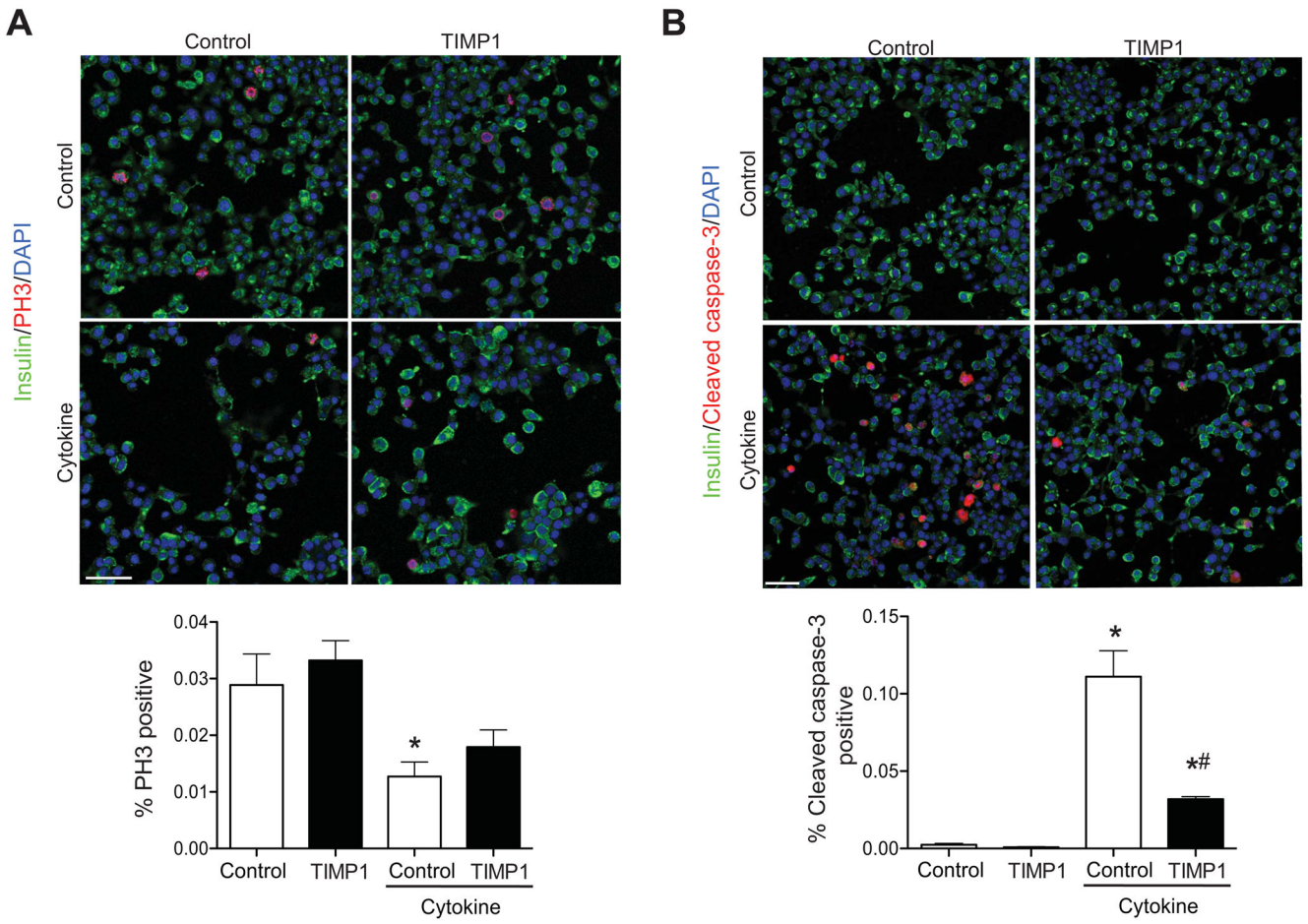

Figure 7. TIMP-1 improves survival of INS-1 β cells treated with proinflammatory cytokines

INS-1 832/13 β cells were treated with or without TNF-α, IFN-γ, and IL-1β and with or without recombinant TIMP-1. Numbers of cells staining positive for PH3 (A) and cleaved caspase-3 (B) were counted and expressed as a percentage of total cell number. Results are expressed graphically and representative images from 3 independent experiments are displayed. *$p<0.05$ compared to cytokine- and TIMP-1-untreated control INS-1 cells. $^{\#}p<0.05$ compared to cytokine-treated INS-1 cells. Scale bars = 50 μm.